Polyimide-Planarized Vertical-Cavity Surface-Emitting Lasers With 17.0-GHz Bandwidth

A. N. AL-Omari, Student Member, IEEE and K. L. Lear, Member, IEEE

Abstract—High-speed oxide-confined polyimide-planarized 850-nm vertical-cavity surface-emitting lasers exhibit —3-dB modulation bandwidths up to 17.0 GHz. The devices are fabricated using a reproducible, simple process incorporating polyimide with good adhesion that does not require implantation or semiinsulating substrates to achieve low capacitance.

Index Terms—Modeling, modulation bandwidth, pad capacitance, polyimide, semiconductor lasers, vertical-cavity surface-emitting lasers (VCSELs).

I. INTRODUCTION

HREE approaches to greater local area network (LAN) link bandwidth are parallel fiber ribbons, wavelength-division multiplexing, and faster single-channel modulation rates. Because vertical-cavity surface-emitting lasers (VCSELs) are widely used in shortwave length (~850 nm) LAN transmitters, it is of interest to develop high-speed VCSELs for faster single-channel systems.

Principal factors affecting laser diode modulation rates are the relaxation oscillation frequency, optical nonlinearities, and parasitic circuit effects that include junction and pad capacitance and distributed Bragg reflector (DBR) series resistance [1]. A very high 70-GHz relaxation oscillation frequency was observed using an electrically pulsed VCSEL [2]. Also, optical nonlinear gain limits the bandwidth of VCSELs by inhibiting high resonance frequencies [1], [3].

Large extrinsic parasitic circuit element values can restrict the maximum modulation bandwidth and, thus, prevent achieving the intrinsic frequency limits. Parasitic circuit elements related to VCSEL die fabrication are mirror and other series resistances and junction, mesa, and bonding pad capacitance. Additionally, wire bond inductance and feed-through capacitances must be considered in packaged devices, although only unpackaged devices were investigated in the work presented here. To maximize the potential modulation rate, the frequency response of the two-port extrinsic parasitic circuit model should have a -3-dB bandwidth somewhat higher than the intrinsic laser bandwidth.

Many researchers have reported methods for reducing parasitic resistances and capacitances associated with VCSELs. Work on reduced series resistance is motivated not only by mod-

Manscript received June 24, 2003; revised September 18, 2003. This work was supported in part by the Mission Research Corporation and Defense Advaned Research Projects Agency under contract DAAD19-03-1-0059.

The authors are with the Electrical and Computer Engineering Department, Colorado State University, Fort Collins, CO 80523 USA (e-mail: ahmad@engr.colostate.edu; kllear@engr.colostate.edu).

Digital Object Identifier 10.1109/LPT.2004.824622

ulation bandwidth concerns, but also initially by issues relating to power efficiency and internal heating. Approaches to lower series resistance contributed by semiconductor mirrors include various forms of compositional grading [4], delta or modulation doping [5], or laterally contacted or other modified VCSEL structures [6]. For the present work, low series resistances have been obtained using previously reported epitaxial mirror designs and p-type substrates [7]. Efforts to reduce VCSEL capacitance have also been reported based on reduction of pad area [1], mesa implantation [8], and semiinsulating substrates. These approaches add complexity such as the need for implantation or deep etches completely through a ~ 10 - μ m epitaxial stack. This letter presents work on low capacitance VCSELs with modulation bandwidths of 17.0 GHz based on a simplified robust process incorporating photosensitive polyimide with good metal adhesion. The process does not require ion implantation, deep field etches to semiinsulating substrates and subsequent metal step coverage, or very small pad areas.

II. FABRICATION

Top-emitting high-speed 850-nm VCSELs were fabricated from an AlGaAs structure on a p-type substrate [7] grown by MOCVD from an epitaxial wafer supplier. The active region contains four GaAs–Al $_{0.2}$ Ga $_{0.8}$ As quantum wells. The n-mirror above the active region is a 20-period 130.65-nm-thick silicon-doped Al $_{0.92}$ Ga $_{0.08}$ As–Al $_{0.16}$ Ga $_{0.84}$ As DBR. The carbon-doped 35-period p-mirror below the active region also employs Al $_{0.92}$ Ga $_{0.08}$ As–Al $_{0.16}$ Ga $_{0.84}$ As compositions except for a single low index $\sim \lambda/4$ layer adjacent to the cavity with 98% instead of 92% Al content.

A processing sequence using six photomasks was utilized to fabricate oxide-confined polyimide-planarized VCSELs with coplanar wave-guide probe pads. Device fabrication began with the formation of cylindrical mesas 28 to 50 μ m in diameter by etching the surrounding semiconductor to a depth of 5 μ m into the bottom p-type mirror using a load-locked CAIBE dry-etching system. To form the current aperture and provide lateral index guiding to the lasing mode, the sample was wet-oxidized in a 440 °C steam environment for 10 min [9]. The oxidation rate was $\sim 1.0 \ \mu \text{m/min}$ for the Al_{0.98}Ga_{0.02}As layer resulting in the oxide extending in 10.5 μ m from the mesa sidewall. Accurate control of oxidation process parameters including water bath temperature, sample temperature, and gas flow rate resulted in a repeatable process and nominally identical oxide-confined VCSELs. Au-Ge-Ni-Au with thicknesses of (670/330/300/70) Å were evaporated in sequence for the annular n-type contact on top of the mesa. Before depositing

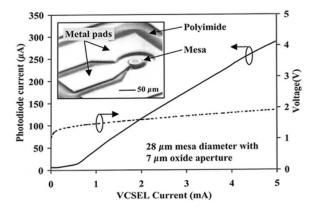


Fig. 1. Photodiode current and VCSEL voltage versus VCSEL bias current.

the bottom p-type contact, the sample was soaked for 15 sec in $HCl-H_2O$ (1:1) solution to remove the $Al_{0.92}Ga_{0.08}As$ surface or the oxide layer formed on the Al_{0.16}Ga_{0.84}As surface. BeAu(prealloyed)–Ti–Au with thicknesses of (500/300/700) Å were evaporated onto the partially etched bottom mirror to form the p-type contact which is connected to the substrate. Contacts were alloyed for 30 sec at 420 °C. After contact formation, photosensitive polyimide was spun on the sample for field insulation and planarization. The central portion of the mesa top as well as a via for the lower p-type contact were exposed and developed prior to curing the polyimide at 350 °C for 30 min in a nitrogen atmosphere. Polyimide planarization offers lower interconnect and pad capacitance than conventional oxide or nitride passivation since it has a lower dielectric constant and can readily produce thick layers, 5.5 μ m after curing in this case. Ti-Au with thicknesses of (200/3000) Å was deposited for metal interconnects and coplanar waveguide probe-bond pads. Heat treatment after the metal deposition was utilized to improve metal-to-polyimide adhesion strength. Further details on polyimide planarization of VCSELs and heat treatments to improve metal-to-polyimide adhesion strength will be published elsewhere. The inset shown in Fig. 1 shows a scanning electron microscope photo for a completed high-speed VCSEL ready for testing.

III. TESTING

The dc characteristics of completed VCSELs were measured using a probe station, an HP 4145A semiconductor parameter analyzer, and a silicon photodiode with a $10 \times 10~\text{mm}^2$ active area and $\sim \! 0.6\text{-A/W}$ responsivity at $\lambda = 850~\text{nm}$. Fig. 1 shows the characteristics of a VCSEL with a $28\text{-}\mu\text{m}$ diameter mesa and $7\text{-}\mu\text{m}$ diameter oxide-confined aperture. The threshold voltage and current were as low as 1.5~V and 0.4~mA, respectively, with a series resistance of $98~\Omega$.

The ac measurement apparatus consisted of a probe station equipped with a 20 °C constant temperature chuck and Cascade Microtech air coplanar probes, \sim 2 m of multimode fiber, a NIST calibrated, high-speed New Focus photodiode and attached New Focus amplifier, an HP 4145 semiconductor parameter analyzer, and an HP8510B vector network analyzer. The bare end fiber was actively aligned above the device under test using an x-y-z positioning stage to obtain maximum dc optical power. The system modulation response S_{21} and laser's microwave reflection coefficient S_{11} were measured

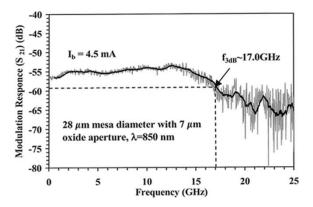


Fig. 2. VCSEL modulation response.

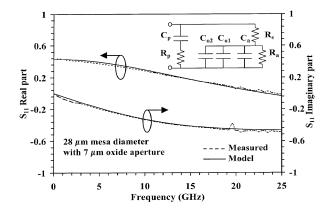


Fig. 3. Real and imaginary S_{11} parameter versus frequency from model and measured data.

for different diameter VCSELs at various bias currents over a frequency range of 100 MHz to 26.5 GHz. As shown in Fig. 2, the 7- μ m diameter aperture laser exhibits a very flat modulation response with a 17.0-GHz bandwidth when biased at $I_b = 4.5$ mA at room temperature. Larger devices exhibit smaller 3-dB frequencies. Mesa diameters of 40 and 50 μm corresponding to 19- and 29- μ m oxide aperture diameters yielded maximum bandwidths of 13.8 and 8.9 GHz, respectively. The moderate bias current densities, such as 11.7 kA/cm² necessary for the 17.0-GHz bandwidth in the 7- μ m diameter device, should improve reliability. The highest VCSEL modulation bandwidth previously published in refereed technical literature was 16.3 GHz [10] although a 21.0-GHz bandwidth using a combined implanted-oxidized device has been reported in conference proceedings [8]. The bias current densities required to achieve these two bandwidths were 50 and 30 kA/cm², respectively.

IV. EQUIVALENT CIRCUIT ANALYSIS

An equivalent circuit for the VCSEL impedance is useful for analysis of both bandwidth limitations of the laser and matching to driver circuits. The circuit model, shown in the inset of Fig. 3, consists of elements corresponding to physical features of the VCSEL die. The contributions to capacitances are represented in Fig. 4. C_a is the aperture's junction capacitance; C_{o1} and C_{o2} represent the mesa regions with single and multiple oxidized layers, respectively, and C_p denotes the pad capacitance between the metal interconnect on the polyimide and the bottom p-mirror stack. R_p is the associated resistance of the remaining

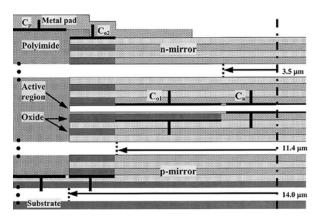


Fig. 4. High-speed VCSEL cross section.

$I_b(mA)$	0.0	1.0	2.0	3.0	4.0	4.5
$R_a(\Omega)$	œ	98.9	85.3	75.9	66.0	64.4
C_{m} (fF)	109	117	125	135	144	151

p-mirror stack under the pad, R_a corresponds to the aperture's junction resistance, and R_s models the series mirror resistances in the mesa.

The pad and combined mesa capacitance values estimated from simple geometrical considerations illustrated in Fig. 4 are in reasonable agreement with parameters extracted by fitting S_{11} data. Note that C_{o1} and C_{o2} contain contributions from the series capacitance of the junction or other intervening depletion regions. The estimated values of C_a , C_{o1} , and C_{o2} , were calculated to be 26.1, 114.4, and \sim 1.9 fF, respectively, for a combined total mesa capacitance of $C_m = 142.4$ fF. The capacitance of the approximately $80 \times 130 \ \mu m$ pad on a 5.5- μm -thick polyimide planarization layer with a relative permittivity of $\varepsilon_r =$ 3.4 is calculated to be 56.9 fF. The incorporation of the polyimide layer results in this capacitance for a conventionally sized $10\,400~\mu\text{m}^2$ pad. Other researchers [1] have published their approach of reducing the size of a bond pad sitting on implanted GaAs to an area of 400 μ m² to obtain a pad capacitance of 0.5 pF and a -3-dB modulation bandwidth of approximately 7.9 GHz.

Measured values of the circuit elements were extracted by fitting both the amplitude and the phase of S_{11} from 100 MHz to 26.5 GHz. Fig. 4 shows measured and fitted data for a 7- μ m oxide aperture VCSEL. Convergence of the fitting values to physically reasonable values was enhanced using the following procedure. First, the capacitances were fixed at their calculated values, and the zero bias (where R_a is very large and can be neglected) S_{11} data was fit to obtain just two unknowns, R_p and R_s . Second, the values for R_a were extracted by fitting the S_{11} data for different bias currents as listed in Table I which includes also extracted values for C_m at different bias currents. Finally, all the circuit parameters were allowed to vary about these values in order to minimize the squared error. The resulting extracted parameters were $R_p = 17 \Omega$, $R_s = 45 \Omega$, $C_p = 62$ fF, and $C_m = 109$ fF, in reasonable agreement with the calculated values. The difference between estimated and extracted C_m may be due to uncertainty in the doping level and, thus, junction depletion capacitance, error in the oxide dielectric constant, and neglecting the narrow depletion region below the thin oxide aperture. Also, the diffusion capacitance was neglected in this estimation.

The 3-dB frequency of the extrinsic equivalent circuit model for the 7- μ m diameter aperture VCSEL driven from a 50- Ω source was found to be 30.7 GHz, indicating that the 17.0-GHz modulation bandwidth is not limited by parasitic circuit effects. From the equivalent circuit, we have found that the parasitic contact pad capacitance C_p that is the same for all lasers is no longer limiting the VCSELs modulation bandwidth as reported in [1].

V. SUMMARY

We have fabricated and characterized high-speed oxide-confined VCSELs with excellent performance using a process without implantation or semiinsulating substrates. The use of photosensitive polyimide gives reliable and repeatable results. The modulation bandwidth of VCSELs with conventionally sized pads is as high as 17.0 GHz and is not limited by extrinsic circuit effects. Additional improvements in the intrinsic relaxation oscillation frequency, damping, and thermal management should lead to VCSELs with modulation bandwidths suitable for 40-Gb/s data transmission.

ACKNOWLEDGMENT

The authors gratefully acknowledge the support of R. Smith, the assistance of D. Woodard for mask layout, D. Patel for CAIBE dry-etching, and D. Galt of Cielo Communications, Inc, for ac measurements.

REFERENCES

- [1] A. K. Dutta, H. Kosaka, K. Kurihara, Y. Sugimasa, and K. Kasahara, "High-speed VCSEL of modulation bandwidth over 7.0 GHz and its application to 100 m PCF datalink," *J. Lightwave Technol.*, vol. 16, pp. 870–875, May 1998.
- [2] D. Tauber, G. Wang, R. S. Geds, J. E. Bowers, and L. A. Coldren, "70 GHz relaxation oscillation in vertical cavity surface emitting laser," *IEEE Trans. Electron. Devices*, vol. 39, p. 2652, Nov. 1992.
- [3] R. Olshansky, P. Hill, V. Lanzisera, and W. Powazinik, "Frequency response of 1.3 μm InGaAsP high speed semiconductor lasers," *IEEE J. Quantum Electron.*, vol. 23, pp. 1410–1418, Sept. 1987.
- [4] K. L. Lear and R. P. Schneider, "Uniparabolic mirror grading for vertical cavity surface emitting lasers," *Appl. Phys. Lett.*, vol. 68, pp. 605–607, 1996
- [5] K. Kojima et al., "Reduction of p-doped mirror electrical resistance of GaAs/AlGaAsvertical-cavity surface-emitting lasers by delta doping," Electron. Lett., vol. 29, no. 20, pp. 1771–1772, Sept. 1993.
- [6] R. A. Morgan et al., "Novel hybrid-DBR single mode controlled GaAs top-emitting VCSEL with record low voltage," in Proc. 7th Annu. Meeting Lasers and Electro-Optics (LEOS'94), Boston, MA, 1994, Extended Abstract PD1.6.
- [7] K. L. Lear *et al.*, "Vertical cavity lasers on p-doped substrates," *Electron. Lett.*, vol. 33, no. 9, pp. 783–784, Apr. 1997.
- [8] —, "Small and large signal modulation of 850 nm oxide-confined vertical-cavity surface-emitting lasers," Advances in Vertical Cavity Surface Emitting Lasers in Trends in Optics and Photonics Series, vol. 15, pp. 69–74, 1997.
- [9] K. D. Choquette et al., "Fabrication and performance of selectivily oxidized vertical-cavity lasers," *IEEE Photon. Technol. Lett.*, vol. 7, pp. 1237–1239, Nov. 1995.
- [10] K. L. Lear et al., "High-frequency modulation of oxide-confined vertical cavity surface emitting lasers," *Electron. Lett.*, vol. 32, pp. 457–458, 1996.